Journal of Visualization, Vol. 2, Nos. 3/4 (2000) 371-380

Holographic Interferometric Visualization of the Richtmyer-Meshkov Instability Induced by Cylindrical Shock Waves

Hosseini, S. H. R.*, Ogawa, T.* and Takayama, K.*

* Shock Wave Research Center, Institute of Fluid Science, Tohoku University 2-1-1, Katahira, Aoba, Sendai 980-8577, Japan.

Received 15 July 1999.
Revised 24 September 1999.

***Abstract*:** Results of quantitative holographic interferometric flow visualization of cylindrical interface instability induced by converging cylindrical shock waves are reported. Experiments were conducted in an annular vertical co-axial diaphragmless shock tube, in which cylindrical soap bubbles filled with He, Ne, Air, Ar, Kr, Xe and SF_6 were co-axially placed in its test section. Pressure histories at different radii during the shock wave implosion and reflection from the center were measured. Diagnostic method base on double exposure holographic interferometry was applied for the measurement of turbulent mixing zone at the interface. The observed cylindrical interfaces were found to have a higher growth rate of turbulent mixing zone than that of the plane shock / plane interface.

***Keywords*:** converging cylindrical shock waves, Richtmyer-Meshkov instability, holographic interferometry, vertical shock tube.

1. Introduction

When a shock wave collides an interface between two gases, a variety of fluid motions is generated, the shock-induced interfacial instability appears during and after its interaction, which is known as shock-excited Rayleigh-Taylor (RT) instability (Rayleigh, 1900; Taylor, 1950) or Richtmyer-Meshkov (RM) instability (Richtmyer, 1960; Meshkov, 1969). The coupling between the pressure gradient across the shock wave and the entropy gradient across the interface, induces baroclinic force which comprises an efficient mechanism for enhancing vorticity. After the shock interaction, the growth of the interface perturbations induces secondary instabilities such as the Kelvin-Helmholtz instability, leading to turbulent mixing between two gases.

The RM instability has been intensively studied experimentally, numerically and analytically. Nevertheless, the interaction of converging and diverging shock waves with interface have not yet been studied experimentally. Since converging shock waves are usually referred to be unstable in the sense that the initial disturbances are amplified with the shock wave convergence (Takayama et al., 1987; Watanabe and Takayama, 1991) and it is technically difficult to produce converging cylindrical shock waves without initial disturbances, little is known about the behavior of a cylindrical interface imposed by a converging cylindrical shock wave. The applications of the problem, such as inertial confinement fusion (ICF) capsule design, turbulent mixing in supersonic combustors, laser fusion, impact welding, and supernova explosions in astrophysics, made it of considerable interest. In ICF the turbulent mixing is undesirable, the interface should remain as smooth as possible with shock wave loading parallel to interface. In this case, the interface thickness is quickly broadened and random small-scale interfacial disturbances grow rapidly to the nonlinear regime.

Most previous RM instability experiments were conducted in conventional shock tubes with various sizes and shock wave impingement on the slightly perturbed or planar shaped gaseous interfaces were studied. However, in previous experiments the effect of wave reflections from shock tube walls, to which the gaseous interface was set perpendicularly, on the process of interfacial instability is not clear. The present work is intended primarily to minimize effects of wave reflection from the wall by considering the interaction of converging and diverging shock waves with cylindrical gaseous interfaces.

In order to investigate the physical behavior of interfacial instability and the induced turbulent mixing zone (TMZ), among various diagnostic techniques, flow visualization is found to be particularly useful. In the present research holographic interferometric flow visualization for the first time was applied to the RM instability. Holographic interferometric visualization enabled to observe quantitatively the flow structure behind the transmitted converging and diverging shock waves after their interaction with interface. Experiments were conducted in an annular vertical diaphragmless shock tube, which is capable of producing converging cylindrical shock waves. Smooth interfaces produced by cylindrical soap bubbles, which ruptured in a relatively ideal manner. The early time growth rate after converging shock wave loading against either light/heavy or heavy/light gaseous interfaces were observed.

2. Experimental Facility and Method

The experiments were conducted in an annular vertical strut-free diaphragmless shock tube. Figure 1 shows its structure. This shock tube has a vertical self-sustained structure and produces cylindrical shock waves with minimum initial disturbances for wide range of shock Mach numbers and with higher degree of repeatability. Its performance characteristics were described in detail by Hosseini et al. (1999).

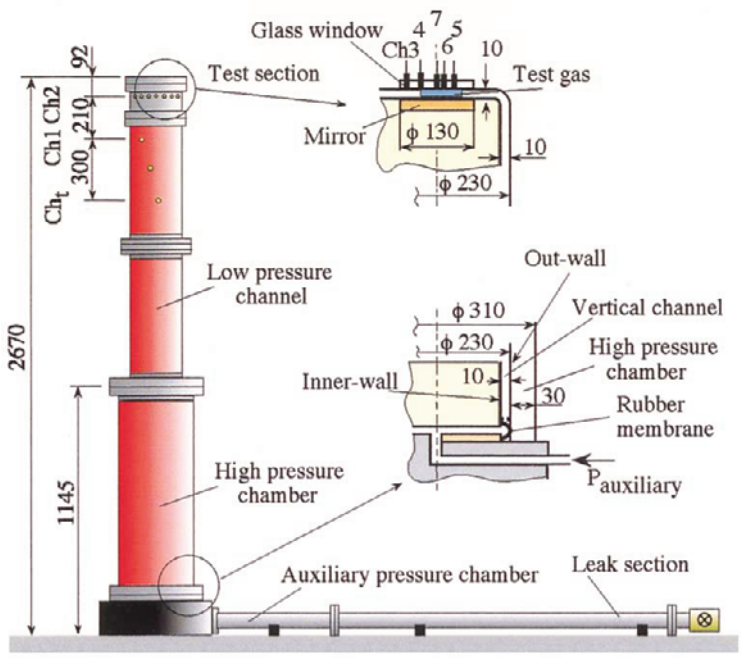

Fig. 1. Structure of annular vertical diaphragmless shock tube.

Pressures were measured by using pressure transducers Kistler model 603B, distributed at locations Ch_1 and Ch_2 along the vertical section, and over the circular converging section at points Ch_3, Ch_4, Ch_5, and Ch_6 with 35 mm, 25 mm, 18.5 mm, and 11.75 mm radius, respectively. Ch_7 was located at the center. Incident shock Mach numbers Ms_i were defined as those measured at 50 mm diameter interfaces.

Figure 2 shows a sketch of the test section. Gaseous interfaces were formed by using soap bubble films, which were made with Plateau's soap solution consisting of 78% distilled water, 20% glycerin, and 2% sodium oleate (Haas and Sturtevant, 1987). The bubble membrane thickness varies, depending on the density of filling gas, from about 0.25 mm for helium to 1.0 mm for SF_6. It is known that interfacial materials separating gases can

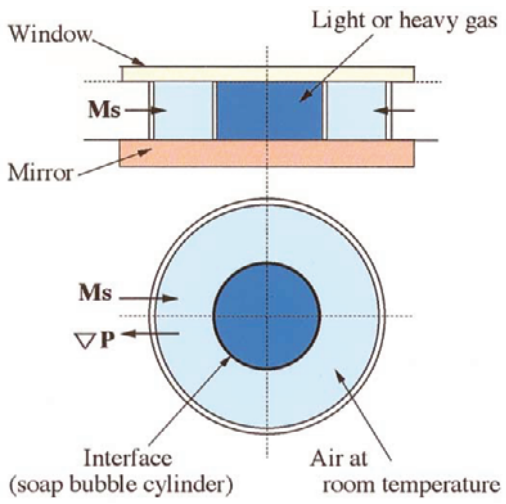

Fig. 2. Test section configuration with cylindrical soap bubble.

change the growth rate of the interface by transferring some part of shock energy to shatter the interface materials. In the case of solid membrane, its shattered fragments are accelerated with the flow and eventually affect the interfacial growth rate. In the present experiments to reduce this nuisance, cylindrical soap bubbles are used, which can be ruptured in a relatively ideal manner. Care was taken to produce very thin and stable cylindrical soap bubbles. Soap solution and test gas were injected with two 0.8 mm i. dia. stainless steel tubes inserted through holes at the 90 degrees bend. The holes were later filled with metal plugs to retain the smooth wall surface. The bottom wall was marked at 50 mm dia. so as to blow the soap bubble exactly to this diameter. The bubble maintained its cylindrical shape between the window and the mirror without deformation for several minutes.

Double exposure holographic interferometry was used for quantitative flow visualization (Takayama, 1983). Figure 3 shows a schematic diagram of the present optical set-up. The optical arrangement consists of two paraboloidal schlieren mirrors and a beam splitter BS which transmitted 60% of source light intensity to an object beam OB and 40% to a reference beam RB. Mirrors M and lenses L were used to make the light path lengths of OB and RB identical with each other. The light source was a holographic double pulse ruby laser (Apollo Laser Inc. 22HD, 25 ns pulse duration, 2 J per pulse). The first laser exposure was triggered by an output signal of pressure transducer Ch_t and was carried out before arrival of the shock wave to the test section and the second exposure was synchronized with the arrival of shock wave at the test section with a proper delay time. Hence, the whole sequences of the cylindrical shock/interface interaction were successfully observed.

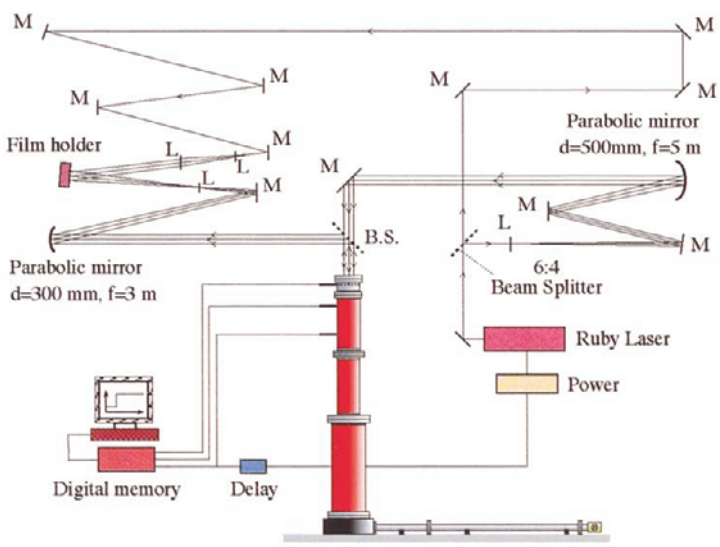

Fig. 3. A schematic diagram of holographic interferometric optical arrangement.

3. Results and Discussion

3.1 Pressure Measurements

Time variation of pressures, normalized by the initial pressure, are shown in Fig. 4 for two different runs, one without bubble and the other with 50 mm dia. air bubble, at incident shock Mach number Ms_i=1.24 in air. Good agreement between these two cases were obtained. This implies that the interface is thin enough to absorb very little energy and its existence is negligibly small, also shows higher degree of repeatability of the shock Mach numbers in this vertical shock tube. Same result was obtained for higher shock Mach number of Ms_i=1.41.

Figure 5 shows the normalized pressure histories of cylindrical shock wave interaction with 50 mm dia. He and SF_6 cylindrical soap bubbles at Ms_i=1.24 in air. In the case of He, as seen in Fig. 5(a), the transmitted shock wave inside He bubble is initially weak and then increases in strength by shock convergence toward the center. The reflected wave from the interface is a rarefaction wave. The sound speed measured in the He cylindrical bubble was 866 m/s whereas it is 999 m/s for pure helium. This infers that the He bubble was contaminated with air. The sound speed of air contaminated helium corresponds to mole fraction 5.6% of air and 94.4% of helium. In the case of SF_6, as seen in Fig. 5(b), the transmitted shock wave is strong and the reflected wave from interface is a shock wave. For both cases the transmitted shock wave converged toward the center.

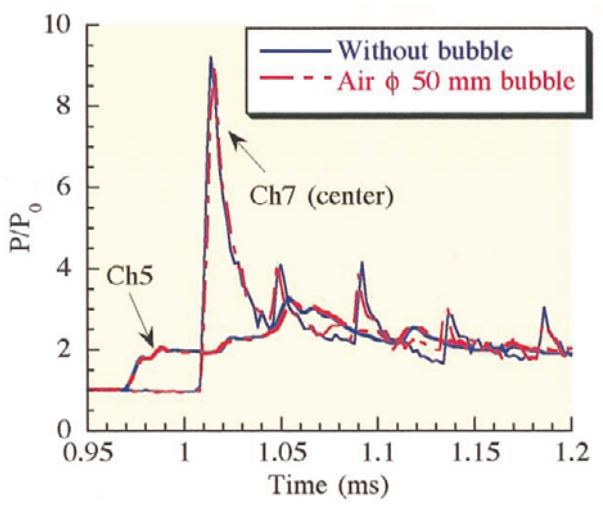

Fig. 4. Comparison of pressure histories measured at the test section for 50 mm dia. air bubble and without bubble, Ms_i=1.24 in air, at initial pressure 102.06 kPa.

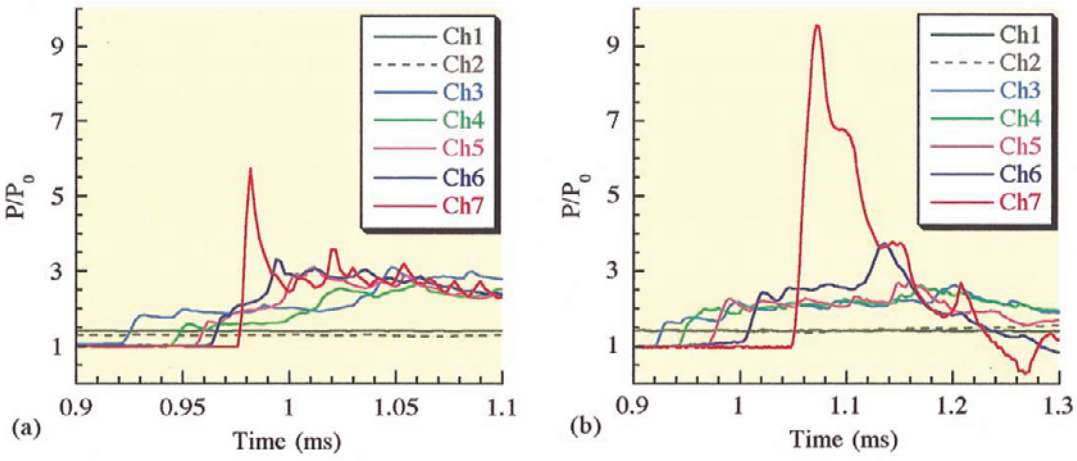

Fig. 5. Pressure histories measured at the test section: (a) He bubble, Ms_i=1.24 in air, initial pressure =100.55 kPa; (b) SF_6 bubble, Ms_i =1.24 in air, at initial pressure =101.77 kPa.

Figure 6 shows the normalized pressure histories at the center of convergence at Ms_i=1.24 in air after interacting with 50 mm dia. He, Ne, air, Ar, Kr, Xe, and SF_6 cylindrical bubbles. Figure 7 shows the variation of central pressures with interfacial post-shock Atwood number A', which is defined by,

$$A' = \frac{\rho'_2 - \rho'_1}{\rho'_1 + \rho'_2}, \tag{1}$$

where ρ'_1 and ρ'_2 are post-shock densities across the interface. In Fig. 7, the transmitted shock Mach numbers inside 50 mm dia. bubbles are shown. The pressures at the center increased by increment of test gas post-shock Atwood number from He (94.4% helium and 5.6% air by volume) up to Kr and then reduced in Xe and considerably in SF_6, which is related to instability of the converging cylindrical shock waves. The cylindrical shock waves were distorted at the interfaces and the small perturbations were generated on the shock shape, which were amplified with the shock wave convergence and became dominant for heavier gases of Xe and SF_6. The experimental result shows strong effect of Atwood number, and the dominant mechanism limiting the maximum pressures and temperatures attainable at the center is the instability of the converging cylindrical shock waves.

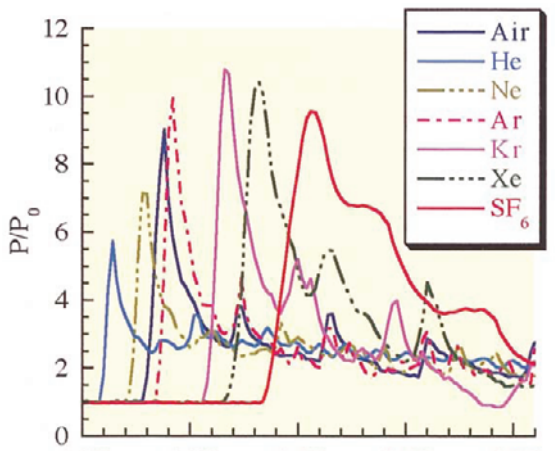

Fig. 6. Measured pressures at the center of convergence versus arrival time of cylindrical shock wave *Ms*=1.24 in air at 50 mm dia. cylindrical interface.

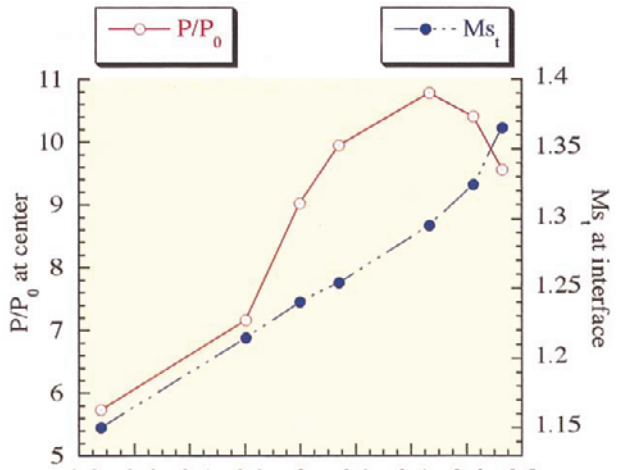

Fig. 7. Variation of pressures at the center and transmitted shock Mach numbers with post-shock Atwood number.

3.2 Wave Diagrams

The wave diagram of the interaction of converging cylindrical shock wave Ms_i=1.24 with 50 mm dia. air/SF_6 cylindrical interface is shown in Fig. 8. The experimental data were obtained from successive pressure measurements as seen in Fig. 5(b), and from sequential holograms. At t = 0 μs cylindrical shock wave impinges the interface and a transmitted converging shock wave of Ms_t=1.365 appears inside SF_6 and a reflected diverging shock wave in air. The transmitted shock wave increases in velocity by shock convergence, and is in good agreement with the prediction obtained from the Whitham's (1973) ray shock theory using Duong and Milton (1985) assumption of the ray tube integral. The agreement of shock velocity for the experiments and the ray shock theory implies that in SF_6 bubble air contamination is negligible. After shock wave reflection from the center at 120 μs, the diverging shock wave collides the interface at 173 μs and a shock wave appears in air and a rarefaction wave in SF_6. The interfacial velocity is not constant. The flow behind the transmitted converging shock wave slightly decelerates the motion of the interface as it moves toward the center. At the moment of diverging shock interaction which is called re-shock at 173 μs, the interface converges to an average diameter of 26.3 mm so that the SF_6 bubble is compressed by a volume ratio of 0.277.

Figure 9 shows the wave diagram of converging cylindrical shock wave Ms_i=1.24 interaction with a 50 mm dia. air/He bubble. The experimental data were obtained from sequential holograms and pressure measurement in Fig. 5(a). At t = 0 ms the cylindrical shock wave impinges the interface and a transmitted converging shock of Ms_t

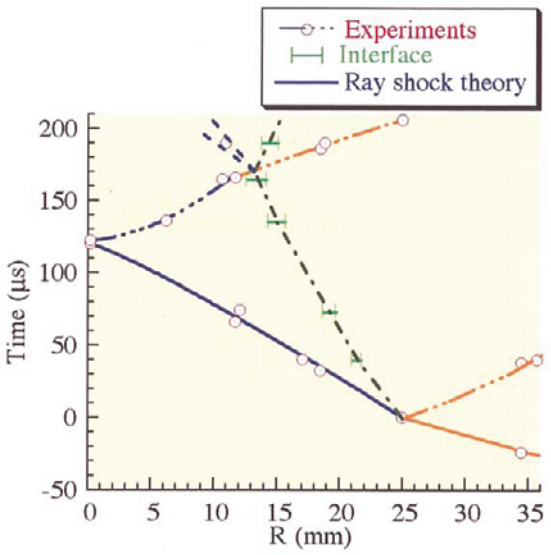

Fig. 8. Wave diagram for interaction of cylindrical shock wave *Ms*=1.24 with air/SF_6 interface.

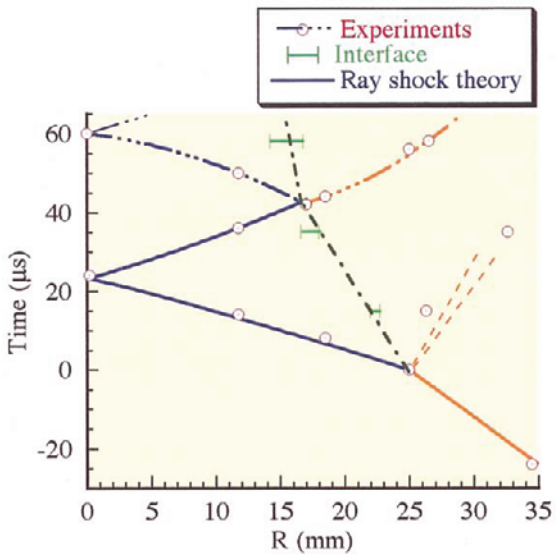

Fig. 9. Wave diagram for interaction of cylindrical shock wave *Ms*=1.24 with air/He interface.

=1.15 appears inside He bubble and a reflected rarefaction wave in air. The velocity of converging cylindrical shock wave agrees well with the prediction of the ray shock theory for He (94.4% helium and 5.6% air by volume). After shock reflection at the center at 23 μs, the diverging shock wave collides the interface at 42 μs, resulting in a transmitted shock wave in air and a reflected converging shock wave in He. At the moment of re-shock of 42 μs, the interface has an average diameter of 33.7 mm and the He bubble is compressed by a volume ratio of 0.454.

3.3 Interferograms

Figure 10 shows sequential infinite fringe interferograms of air/SF_6 interface after interaction with cylindrical shock wave Ms_i=1.24 in air at 102.06 kPa. Figure 10(a) shows the 34.3 mm dia. transmitted converging cylindrical shock wave inside the SF_6, the 42.7 mm dia. cylindrical interface which is broadened to 0.78 mm thickness, and the 71.5 mm dia. reflected shock wave from the interface, at 40 μs after shock wave arrival at the interface. The transmitted shock wave in the SF_6 becomes strong due to low sound speed of the SF_6, so that the number of fringes increases inside the SF_6. In Fig. 10(a), the initial position of the 50 mm dia. interface is shown and the dark point in left hand side of the center is remaining of a droplet of soap solution which was used for bubble formation. Figure 10(b), at 136 μs, shows the later time after reflection of the transmitted shock wave from the center. Hardly visible inside the SF_6 is a 12.5 mm dia. diverging cylindrical shock wave. The interface thickness has broadened. Clearly observable density perturbations in the SF_6 bubble are due to the shock distortion during interaction and the growth of small perturbations behind the converging cylindrical shock wave.

Figure 10(c) at 165 μs after arrival of shock wave, shows the interface before interaction with the diverging shock wave. The broadened interface and the 21.4 mm dia. diverging shock are readily observable. The interaction of converging shock wave with the air/SF_6 interface distorted not only the interface but also the shock shape which generated jaggedly shaped fringe distributions. If the shape of converging shock wave is distorted, its perturbation would be amplified with the shock wave convergence. However, it will not grow to catastrophic amplitude but would be stabilized by non-linear stability, that is, large difference in physical variables between two neighboring segments of a shock wave eventually form creation of the Mach reflection. Once Mach reflections appear, pair vortices are also generated at their triple points. The final mergence of the vortices at the center, produce the jaggedly shaped density perturbations behind the reflected diverging shock wave.

Figure 10(d), at 190 μs, shows the interface after interaction with diverging cylindrical shock wave. The bright band inside and near the interface is the reflected rarefaction wave. The relatively strong diverging shock wave compressed the interface and decreased its thickness. It is also well recognized that in gases having smaller ratio of specific heats the interaction of shock wave with the wall boundary layer is so enhanced that the front of

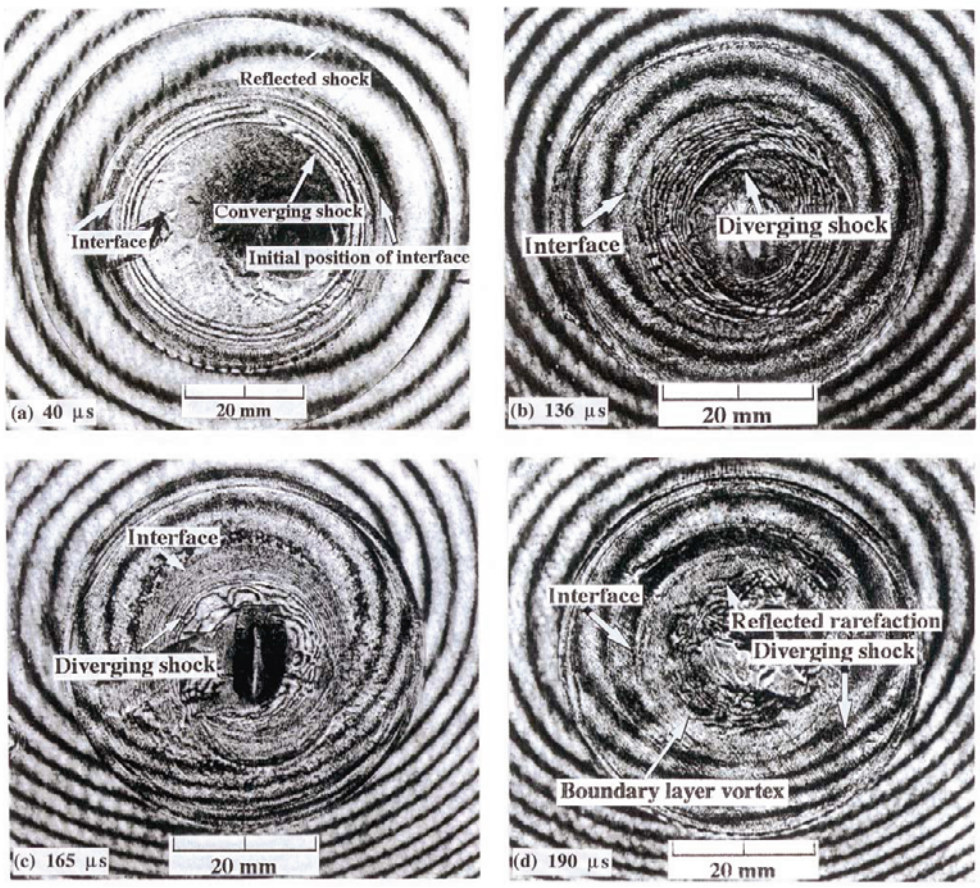

Fig. 10. Infinite fringe holograms of air/SF_6 interfacial instability, Ms_i=1.24±%0.2 in air at 102.06 kPa.

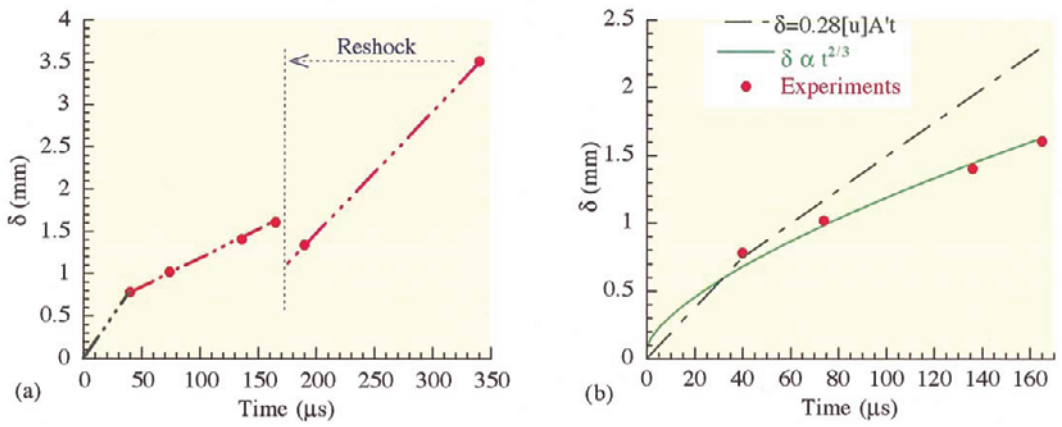

Fig. 11. Time evolution of the TMZ thickness for air/SF_6 interface, Ms_i=1.24±%0.2 in air at 102.06 kPa.

shock wave is often bifurcated. This trend is dominating in the SF_6 bubble and the wall vortex is observed. In Fig. 10(d) the dark point near center is soap solution droplet.

The time evolution of the thickness δ of the turbulent mixing zone (TMZ) for the air/SF_6 interface is shown in Fig. 11. The growth rate induced by converging cylindrical shock wave has an average of 19.5 m/s between t= 0 and 40 μs, and is 6.6 ± 0.3 m/s between t=40 and 165 μs, which shows the rapid and nonlinear growth of small-scale perturbations. The interface thickness increases at 15.2 ± 0.7 m/s in time after arrival of the diverging shock wave at 173 μs. In the present research with cylindrical shock acceleration, the growth rate of air/SF_6 interface

thickness is higher than plane shock / air-SF_6 interface growth reported by previous investigators (Brouillette and Sturtevant, 1989, 1993; Vetter and Sturtevant, 1995). The comparison of the interfacial thickness after the first shock with theory of the total turbulent kinetic energy deposition at interface by the shock wave, $\delta \alpha t^{2/3}$ (Barenblatt, 1983), is shown in Fig. 11(b). The experimental data are compared with Mikaelian's (1989) prediction also. Mikaelian adapted the RT instability experimental results of Read (1984) to the impulsively accelerated interface and obtained a linear time relation for the growth rate of an initially planar interface,

$$\delta = 0.28[u]A't, \tag{2}$$

where $[u]$ and A' are the interface velocity and the Atwood number across the interface based on the post-shock densities, Eq. (1). By considering the variation of interfacial velocity, average of $[u]$ before and after 40 μs are used. As seen in Fig. 11(b), the growth rate at early time is in good agreement with Eq (2). For longer time, after 40 μs, the $t^{2/3}$ power law becomes dominant.

Figure 12 shows sequential infinite fringe interferograms of cylindrical shock wave interaction with air/He interface at Ms_i=1.24 in air at 101.96 kPa. Figure 12(a), 15 μs after shock wave arrival at the interface, shows a reflected rarefaction wave from the interface and a 0.81 mm thickness cylindrical interface, the weak transmitted shock wave in He was not visible. In Fig. 12(a) the initial position of 50 mm dia. interface is marked and the dark spot near the center is remains of soap solution droplet. Figure 12(b), at 70 μs, shows the interface after interaction with diverging cylindrical shock wave. The interaction of diverging shock wave increased the interface thickness. Due to the interaction of diverging shock wave behind the interface a boundary layer vortex with intensified mixing near the wall was induced. Figures 12(c,d) show the later time at 175 μs and 255 μs after arrival of the cylindrical shock wave. The interface thickness completely increased.

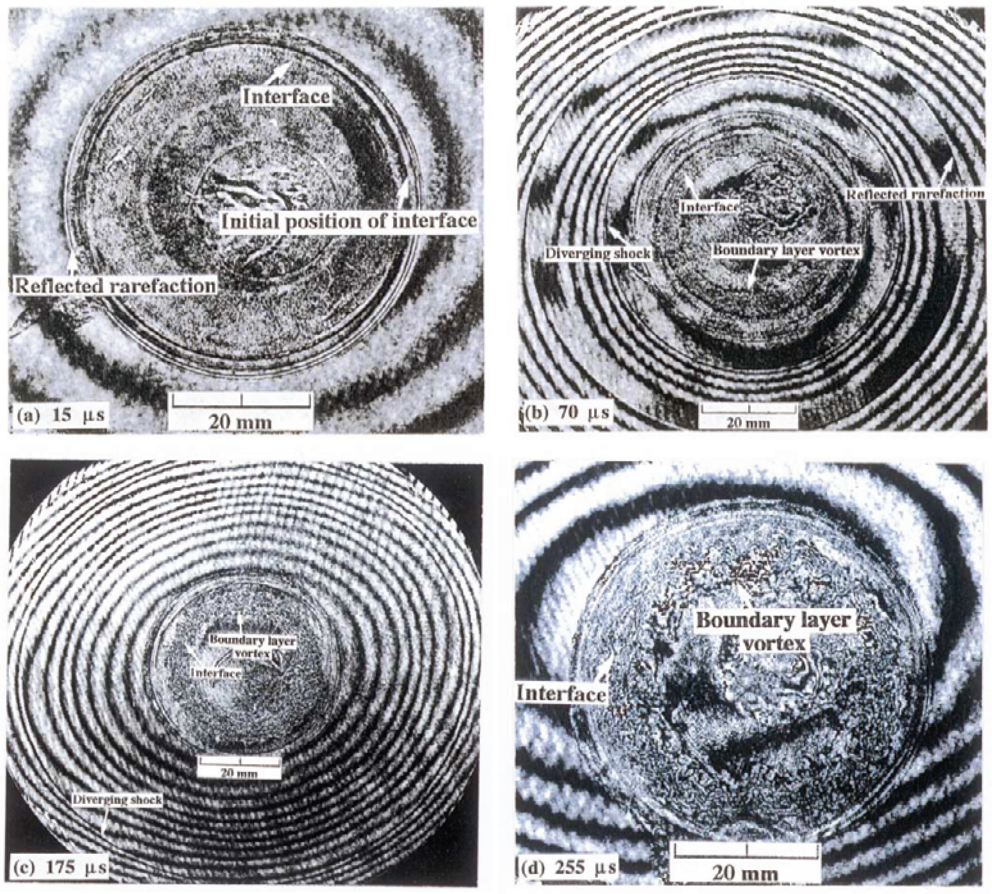

Fig. 12. Infinite fringe holograms of air/He interfacial instability, Ms_i=1.24±%0.2 in air at 101.96 kPa.

Figure 13 shows the time evolution of the thickness δ of the TMZ for the air/He interface. The average growth rate of the interface induced by converging cylindrical shock wave is 40.6±1 m/s. After interaction of diverging shock wave it is 41.7±1 m/s, and is 11.9±1 m/s for late time after repeating several interactions. Since the time duration between cylindrical converging and diverging shock wave interactions is relatively short, 42 μs, the interfacial growth rate after first shock acceleration exhibits a nearly linear variation and is in good agreement with Eq. (2).

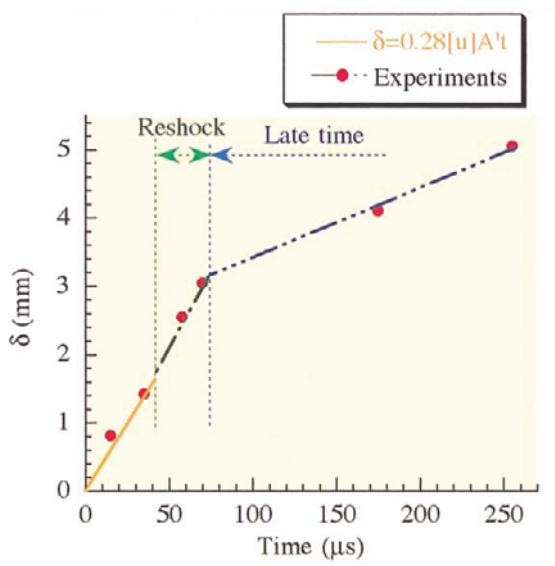

Fig. 13. Time evolution of the TMZ thickness for air/He interface, Ms_i=1.24±%0.2 in air at 101.96 kPa.

4. Conclusions

The obtained results are summarized as follows:

1) The interaction of cylindrical shock waves with cylindrical interfaces in the vertical annular diaphragmless shock tube was studied.
2) Pressure histories at the test section before and after cylindrical shock wave loading of either heavy/light or light/heavy interfaces were measured. The maximum pressures at the center of convergence were compared.
3) Using double exposure holographic interferometric quantitative visualization the flow structure behind the transmitted converging and diverging shock waves after interaction with air/SF_6 and air/He interfaces were observed and the time evolution of the interface thicknesses were verified.
4) The observed cylindrical interfaces had a higher growth rate of TMZ in the present research than that of the plane shock / plane interface reported by previous investigators.

Acknowledgments

The authors wish to express their gratitude to Dr. O. Onodera and Mr. H. Ojima of the Shock Wave Research Center, Institute of Fluid Science, Tohoku University, for their assistance in conducting the experiments. The authors also acknowledge the staff of the machine shop of the Institute of Fluid Science, Tohoku University for their help in manufacturing of the shock tube and the test section.

References

Barenblatt, G. I., Self-similar turbulence propagation from an instantaneous point source, In Non-linear Dynamics and Turbulence, Ed. Barenblatt et al., (1983), 48, Pitman, Boston.

Brouillette, M. and Sturtevant, B., Growth induced by multiple shock waves normally incident on plane gaseous interfaces, Physica D, 37 (1989), 248-263.

Brouillette, M. and Sturtevant, B., Experiments on the Richtmyer-Meshkov instability: Small-scale perturbations on a plane interface, Phys. Fluids A, 5-4 (1993), 916-930.

Duong, D. Q. and Milton, B. E., The Mach-reflection of shock waves in converging cylindrical channels, Exp. Fluids, 3 (1985), 161-168.

Haas, J. F. and Sturtevant, B., Interaction of weak shock waves with cylindrical and spherical gas inhomogeneities, J. Fluid Mech., 181 (1987), 41-76.
Hosseini, S. H. R., Onodera, O. and Takayama, K., Stability of converging cylindrical shock waves in a vertical annular co-axial diaphragmless shock tube, Tran. of the Japan Soc. Aeronautical and Space Sciences, 42-135 (1999), 19-26.
Meshkov, E .E., Instability of the interface of two gases accelerated by a shock wave, Soviet Fluid Dynamics, 4-5 (1969), 101-108.
Mikaelian, K. O., Turbulent mixing generated by Rayleigh-Taylor and Richtmyer-Meshkov instabilities, Physica D, 36 (1989), 343-356.
Lord Rayleigh, In Scientific Papers, Vol II (1900), 200, Cambridge University Press, Cambridge, England.
Read, K. I., Experimental investigation of turbulent mixing in Rayleigh-Taylor instability, Physica D, 45 (1984), 45-58.
Richtmyer, R. D., Taylor instability in shock acceleration of compressible fluids, Comm. Pure and Applied Math., XIII (1960), 279-319.
Takayama, K., Kleine, H. and Grönig, H., An experimental investigation of the stability of converging cylindrical shock waves in air, Exp. Fluids, 5 (1987), 315-322.
Takayama, K., Application of holographic interferometry to shock wave research, Proc. SPIE, 398 (1983), 174-181.
Taylor, G.I., The instability of liquid surfaces when accelerated in a direction perpendicular to their planes, I, Proc. Roy. Soc. London Ser. A, 201 (1950), 192-196.
Vetter, M. and Sturtevant, B., Experiments on the Richtmyer-Meshkov instability of air/SF_6 interface, Shock Waves, 4 (1995), 247-252.
Watanabe, M. and Takayama, K., Stability of converging cylindrical shock wave, Shock Waves, 1 (1991), 149-160.
Whitham, G.B., Linear and Nonlinear Waves, (1973), 263-311, Wiley-Interscience.

Author Profile

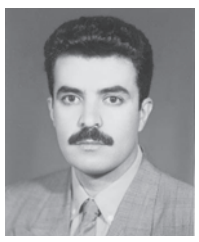

Seyed Hamid Reza Hosseini: He received his M.Sc. (Eng.) degree in Mechanical Engineering in 1990 from Sharif University of Technology, and his Ph.D. in Aeronautics and Space Engineering in 1999 from Tohoku University. Before starting of his Ph.D. he was lecturer in the School of Mechanical Engineering of Sharif University of Technology. After the Ph.D., he has been postdoctoral researcher supported by the Japan Space Forum, and then he has been promoted to be a research associate of the Shock Wave Research Center, Institute of Fluid Science, Tohoku University. His research interests are shock wave propagation in non-uniform media, shock waves focusing, and recently in medical applications of shock waves.

Toshihiro Ogawa: He received his Electrical High School Diploma in 1991 from Yokote Technical High School. Since then, he has been working as a technician supporting shock wave experiments in the Shock Wave Research Center, Institute of Fluid Science, Tohoku University. He is mainly working for the operation of diaphragmless shock tubes and for the acquisition of holographic interferograms and their evaluation.

Kazuyoshi Takayama: He received his B.Sc. (Eng.) degree in Mechanical Engineering in 1963 from Nagoya Institute of Technology, his M.Sc. (Eng.) degree in 1965 and his Ph.D. in Mechanical Engineering in 1973 from Tohoku University. In 1986, he was promoted to be a Professor of Tohoku University, and in 1988 was appointed to be a director of Shock Wave Research Center, Institute of Fluid Science, Tohoku University. His primary interests were in basic research of shock wave dynamics. He has succeeded intensive use of double exposure holographic interferometry for shock wave research. Results of these shock wave researches have been successfully applied to various fields of science, technology, and industry.